This article is a *Plant Cell* Advance Online Publication. The date of its first appearance online is the official date of publication. The article has been edited and the authors have corrected proofs, but minor changes could be made before the final version is published. Posting this version online reduces the time to publication by several weeks.

# Actin-Dependent and -Independent Functions of Cortical Microtubules in the Differentiation of *Arabidopsis* Leaf Trichomes[W]

**Adrian Sambade,[a] Kim Findlay,[a] Anton R. Schäffner,[b] Clive W. Lloyd,[a] and Henrik Buschmann[a,1,2]**

[a] Department of Cell and Developmental Biology, John Innes Centre, Norwich Research Park, Norwich, NR4 7UH, United Kingdom
[b] Institute of Biochemical Plant Pathology, Helmholtz Zentrum München, 85764 Neuherberg, Germany

***Arabidopsis thaliana tortifolia2* carries a point mutation in α-tubulin 4 and shows aberrant cortical microtubule dynamics. The microtubule defect of *tortifolia2* leads to overbranching and right-handed helical growth in the single-celled leaf trichomes. Here, we use *tortifolia2* to further our understanding of microtubules in plant cell differentiation. Trichomes at the branching stage show an apical ring of cortical microtubules, and our analyses support that this ring is involved in marking the prospective branch site. *tortifolia2* showed ectopic microtubule bundles at this stage, consistent with a function for microtubules in selecting new branch sites. Overbranching of *tortifolia2* required the C-terminal binding protein/brefeldin A-ADP ribosylated substrate protein ANGUSTIFOLIA1, and our results indicate that the *angustifolia1* mutant is hypersensitive to alterations in microtubule dynamics. To analyze whether actin and microtubules cooperate in the trichome cell expansion process, we generated double mutants of *tortifolia2* with *distorted1*, a mutant that is defective in the actin-related ARP2/3 complex. The double mutant trichomes showed a complete loss of growth anisotropy, suggesting a genetic interaction of actin and microtubules. Green fluorescent protein labeling of F-actin or microtubules in *tortifolia2 distorted1* double mutants indicated that F-actin enhances microtubule dynamics and enables reorientation. Together, our results suggest actin-dependent and -independent functions of cortical microtubules in trichome differentiation.**

## INTRODUCTION

Plant cells specify their shapes with the aid of cytoskeletal systems. The unicellular leaf trichome of *Arabidopsis thaliana* has served as a model for studying the function of microtubule and actin networks in the differentiation of plant cells (Schnittger and Hülskamp, 2002; Smith and Oppenheimer, 2005; Szymanski, 2009). *Arabidopsis* trichomes are erect hair-like structures typically showing three or four straight branches (Marks et al., 1991; Hülskamp et al., 1994). In trichomes, microtubules have two main functions: As in other plant cell types, they are responsible for the regulation of anisotropic cell expansion (i.e., differential expansion of the different axes), but they are also required for cell branching. Both functions are supported by phenotypes obtained by applying antimicrotubule drugs and by various *Arabidopsis* mutants affected in the microtubule cytoskeleton (Torres-Ruiz and Jürgens, 1994; Oppenheimer et al., 1997; Burk et al., 2001; Kirik et al., 2002; Abe et al., 2004; Buschmann and Lloyd, 2008). In the wild type, and at around the time of branch initiation, cortical microtubules gather to form a collar of microtubule bundles in the apical part of the elongating trichome stalk. This collar is assumed to have a function in trichome branching, as supported by results obtained from the underbranched trichome mutant *angustifolia1* (*an1*; Folkers et al., 2002). AN1 is the plant homolog of the C-terminal binding protein/brefeldin A-ADP ribosylated substrate (CtBP/BARS). In *an1* mutants, this array of cortical microtubules is no longer focused at the stalk's tip but is evenly distributed over the flanks of the cell. This suggests that the AN1 protein may have a function in microtubule positioning and that a dense collar of cortical microtubules in an apical position is important for normal branching (Szymanski, 2009). The *AN1* gene encodes the plant homolog of CtBP/BARS and was postulated to function in vesicle budding from the Golgi (Folkers et al., 2002; Kim et al., 2002; Corda et al., 2006; Stern et al., 2007; Bai et al., 2010). Apart from this correlative evidence that the cortical microtubule collar seen in young trichome stalks is required for branching (Folkers et al., 2002), we have little understanding of the microtubule configurations of the exact branch point before and at branching, nor is it known how microtubule arrays are formed and established on the new branch (Beilstein and Szymanski, 2004).

Cortical microtubules of trichomes have the important additional function of facilitating anisotropic cell expansion. At an early stage, when wild-type trichomes have just branched or are as yet unbranched, cortical microtubules orient perpendicularly to the main direction of growth (Mathur and Chua, 2000; Folkers et al., 2002; Buschmann et al., 2009). As in other cell types, it is assumed that cortical microtubules of trichomes align the cellulosic microfibrils of the cell wall (Paredez et al., 2006; Szymanski, 2009). This will channel orthogonally the force generated by turgor pressure, thereby facilitating polar cell expansion. However,

[1] Current address: Department of Biology and Botany, University of Osnabrück, 49076 Osnabrück, Germany.
[2] Address correspondence to henrik.buschmann@biologie.uni-osnabrueck.de.
The author responsible for distribution of materials integral to the findings presented in this article in accordance with the policy described in the Instructions for Authors (www.plantcell.org) is: Henrik Buschmann (henrik.buschmann@biologie.uni-osnabrueck.de).
[W] Online version contains Web-only data.
www.plantcell.org/cgi/doi/10.1105/tpc.113.118273

  

mutational analyses and drug treatment have shown that normal growth anisotropy of the trichome branch also requires an intact actin cytoskeleton. *Arabidopsis* trichome mutants of the *distorted* (*dis*) class have provided a useful system to study actin-dependent cell morphogenesis (Mathur, 2005; Szymanski, 2005). DIS1, for example, encodes an actin-related protein (ARP3) and genetic, cell biological, and biochemical data suggest that DIS1 is a functional member of a plant ARP2/3 complex (Le et al., 2003; Kotchoni et al., 2009; Maisch et al., 2009). The ARP2/3 complex nucleates actin filaments from the side of existing filaments, resulting in microfilament branching. This was shown for the model organism *Acanthamoeba* (Blanchoin et al., 2000; Volkmann et al., 2001); however, in plants, the ARP2/3 complex is found in diverse intracellular localizations (Zhang et al., 2013). The trichomes of the *Arabidopsis dis1* mutant are somewhat swollen and slightly shorter than the wild type, and the direction of growth can change abruptly. Although data obtained from drug application and the phenotypes of various mutants suggest that microtubules and actin are both required for the regulation of anisotropic cell expansion in trichomes and other plant cells, genetic data that demonstrate a clear link between both cytoskeletal systems are currently missing.

We recently analyzed the organ expansion defect in the helical growth mutant *tortifolia2* (*tor2*), whose phenotype is based on the R2K (Arg to Lys) mutation of α-tubulin 4 (Buschmann et al., 2009). The *tor2* mutant shows several distinct defects in the dynamics of cortical microtubules. Many of the observed aberrations argue for microtubules being hyperstabilized in the *tor2* background, which is probably caused by a decreased GTP hydrolysis rate in *tor2* microtubules (Ishida et al., 2007; Buschmann et al., 2009). Interestingly, the *tor2* mutant shows right-handed cell expansion even in the single-celled leaf trichomes. In addition, the trichomes of *tor2* are overbranched. This is consistent with the previous notion that microtubules have two functions in trichomes, namely, elongation and branching, whereas actin functions are required for elongation only (Szymanski et al., 1999). Apparently, microtubules support two separate developmental pathways in trichomes, but little is known about the associated molecular components. In this study, we use the phenotype of *tor2* trichomes to better understand the apparently separate branching and cell elongation functions of microtubules. First, we provide evidence that cortical and not endoplasmic microtubules are important for branch initiation in the wild type. This is supported by confocal microscopy of overbranched *tor2*, where ectopic cortical microtubule accumulations induced additional branch sites. In order to deepen our understanding of microtubule function during branching, we analyzed double mutants of *tor2* with *an1*. The AN1 protein is believed to have a microtubule-related function (Folkers et al., 2002; Kim et al., 2002), but it is unclear how this mutant responds to the specific alterations of microtubule dynamics. Finally, we were interested to understand the similarities and differences of trichome twisting in *tor2* and *dis1* background. The *dis1* phenotype was occasionally described as "twisted" (Hülskamp et al., 1994; Le et al., 2003; Beilstein and Szymanski, 2004), but it is not known whether there is handedness to *dis1* twisting, nor is it clear whether the normal expansion growth leading to straight trichomes requires a functional interaction of actin with microtubules. Our analysis of F-actin and microtubules in the wild type and mutants allows us to extend earlier models on how the branch point is selected, how the early bulge is formed, and how the transition to branch elongation is achieved. Our results also provide genetic evidence for a functional cooperation of microtubules with F-actin in anisotropic cell expansion.

## RESULTS

### Cortical Microtubules Mark the Trichome Branching Site, but the Branch Bulges Out in the Absence of a Conspicuous Microtubule Configuration

There is some evidence that cortical microtubules underlying the plasma membrane are involved in the branching of trichomes (Folkers et al., 2002). To provide support for the idea that cortical microtubules (and not other types of microtubule configurations, such as endoplasmic microtubules) are the basis of branching in trichomes, we analyzed the branching process at increased spatiotemporal resolution. Analyses were performed for the wild type and for overbranched *tor2*. This was done by confocal microscopy using the microtubule markers EB1–green fluorescent protein (GFP) (here, short-term movies were used for t- and z-stack projections as described in Buschmann et al., 2010) and GFP-TUB6 (using z-stack projections). We observed the typical apical collar of cortical microtubules in the elongated but unbranched trichome of the wild type (Mathur and Chua, 2000; Folkers et al., 2002; Beilstein and Szymanski, 2004). Toward the base of the trichome, and at the very tip, microtubule density was reduced (Figure 1A; Supplemental Movie 1). When the new branch became visible, it was formed as a gentle bulge seen just beneath the microtubule collar. Interestingly, the early developing bulge can be devoid of microtubules, or it may show only weak signals without specific microtubule alignments (Figure 1B). In any case, the GFP signal of the bulge at this stage was much lower than the signal for the collar of the same cell. These analyses were done using the EB1-GFP marker (Figure 1); however, early branching trichomes with obvious bulges showing no significant microtubule accumulations were also seen in the GFP-TUB6 marker line (Supplemental Figure 1). Eventually, and as the bulge became bigger, microtubules outlined the incipient tip as a ring, but this ring was initially wide in diameter, up to 10 μm (Figure 1C; Supplemental Figures 2A and 2B). This ring then narrowed as the bulge became a branch (Figures 1D and 1E). The same process was reiterated in secondary branch formation (Supplemental Figures 2C and 2D). We then asked whether internal (endoplasmic) microtubules and/or the nucleus are involved in the branching process. During early trichome development, the nucleus could be seen to ascend out of the plane of the epidermal cell layer into the trichome's main body. However, no microtubules were found connected to the nucleus, and the nucleus always remained at a certain distance (10 to 20 μm) away from, and not at, the emerging trichome branch (Supplemental Figures 2A and 2B). In general, very few endoplasmic microtubules were seen in branching trichomes (Supplemental Movie 2). Taken together, this indicates that when the bulge of the new branch becomes first visible, it is formed beneath the apical microtubule collar. The early

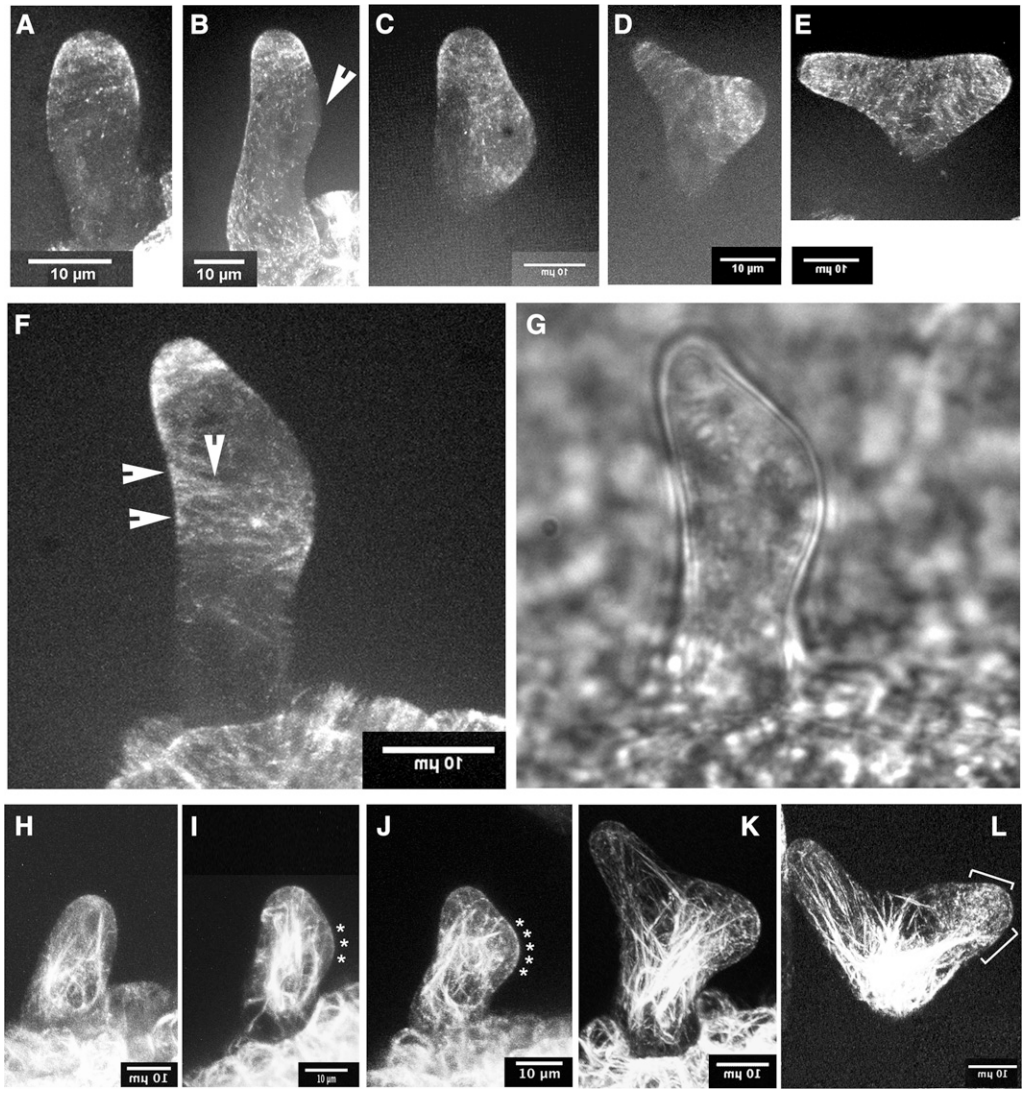


**Figure 1.** The Early Bulge of Wild-Type Trichomes Contains Few Cortical Microtubules but a Conspicuous F-Actin Signal.

Microtubules (**[A]** to **[F]**) were imaged using EB1-GFP, and the data were subjected to t- and z-projections (at least 10 time points each).
**(A)** The microtubule collar seen in trichomes before branching.
**(B)** Trichome cell with collar and first indication of subapical branching (arrowhead). The bulge shows no microtubules.
**(C)** The bulge is now clearly visible and weakly outlined by microtubules; however, its center is devoid of microtubules.
**(D)** and **(E)** As the bulge becomes a branch, an increasingly strong microtubule signal is seen. The new microtubule collar becomes progressively narrower.
**(F)** and **(G)** *tor2* mutant trichome undergoing bulge formation displays prominent ectopic microtubules. Arrows in **(F)** point to ectopic microtubule bundles.
**(H)** to **(L)** Micrographs show a developmental sequence of F-actin organization during trichome branching based on GFP-fABD2 expression.
**(H)** Unbranched trichome.
**(I)** Trichome with early bulge indicating branch formation. Note F-actin signal at center of bulge (asterisks).
**(J)** As the bulge grows, the cortical F-actin signal in its center becomes stronger.
**(K)** Endoplasmic actin cables become connected to distal foci near or at the branch tips.
**(L)** In the new branch, fine F-actin gathers in the region of the tip forming an F-actin cap (brackets).
Bars = 10 μm. Inverted scale bar legends indicate that the panel was mirrored in order to allow all branching events of the figure to point to the right.

bulge shows no, or very few, microtubules, but a second microtubule collar is eventually assembled de novo as a wide ring located at the base of the enlarging bulge. Our results further suggest that cortical microtubules and not other configurations (i.e., endoplasmic microtubules) are important for branching.

In *tor2* trichomes before branching or at the early bulging stage, cortical microtubules were frequently located in aberrant positions (Figure 1F). In unbranched *tor2* trichomes, cortical microtubules were seen to be less focused into a single apical collar and to cover a wider surface. In addition, bundles of

cortical microtubules were frequently observed in ectopic positions separate from the collar. Such microtubule accumulations can cover a considerable fraction of the circumferential cortex of the young trichome cell (Figures 1F and 1G; Supplemental Movie 3).

Genetic and pharmacological data suggest that microtubules and not actin are involved in branch initiation. However, after observing that the early bulge is formed without microtubules, we investigated whether another cytoskeletal network (i.e., F-actin) was present during bulge formation. A study of bulge formation was therefore performed using the improved actin marker line GFP-fABD2 (Sheahan et al., 2004). No obvious accumulation of F-actin at the branch site was detected before bulging (Figure 1H). However, at the first sign of bulge formation, a signal of cortical F-actin was found in the central region of the emerging bulge (asterisks in Figures 1I and 1J). Next, numerous endoplasmic cables of F-actin were formed that reached from the nuclear region toward the tip of the branch (Figure 1K). As the branch became larger, the cortical F-actin signal became stronger and its area enlarged. This produced a "cap" of fine F-actin that extended into the position of the microtubule collar (brackets in Figure 1L; compare with Figures 1D and 1E). The alignment of cortical actin filaments in the F-actin cap was often transverse. Thus, these results indicate that cortical F-actin is first to populate the enlarging bulge in trichome branching. This is followed by localization of cortical microtubules to the same site (compare Figures 1B and 1C with Figures 1I and 1J).

### During Branch Elongation Helical Microtubule Arrays of Defined Handedness Are Seen in the Wild Type

Next, we aimed at following the developmental progression of microtubule alignment from early to late trichome elongation stages. Microtubule orientations of the wild type and *tor2* were measured with respect to the trichome cell axis. The microtubule pattern in elongating but yet unbranched wild-type trichomes was mainly transverse (Figure 2A) but became more complex after branching (Figures 2B and 2C). Elongating branches were classified into early (up to 75 μm) and late (>75 μm) stages. Wild-type microtubule arrays of branches at the early elongating stage (Figure 2B) were found to be transverse or helical, and there was a slight bias toward right-handed microtubule orientation (31.7% right-handed versus 11.7% left-handed; $n = 60$). However, in late-elongating wild-type branches (Figure 2C), a strong bias was detected toward left-handed orientations (64.3% left-handed versus 7.1% right-handed). This preference for left-handed arrays in late-elongating branches of the wild type was confirmed using the alternative microtubule marker GFP-TUB6 (Figure 2D; Supplemental Figures 3A to 3D). In *tor2* trichomes, cortical microtubules showed left-handed orientations at all stages of growth, although this was less pronounced during early branch elongation (Figures 2A to 2C). This left-handed microtubule orientation of *tor2* was also seen using the GFP-TUB6 marker (Figure 2E; Supplemental Figure 3D) and is consistent with the morphological twist seen in *tor2* trichomes (Buschmann et al., 2009). Taken together, this shows that helical microtubule arrays with consistent handedness are not only formed in *tor2*, but also in the wild type. This is surprising, since mature *Arabidopsis* wild trichomes are straight. However, handed microtubule arrays have previously been observed in late elongating wild-type root cells of *Arabidopsis* and maize (*Zea mays*; Liang et al., 1996; Sugimoto et al., 2000). Straight growth of wild-type plants is usually associated with transverse microtubules; however, it appears that when growth decelerates, microtubule orientation can change and arrays of a specific handedness are formed. Apparently this also applies to wild-type trichomes (Figure 2C).

Finally, we investigated how microtubules align after growth has ceased. A recent report showed that in the epidermis of *Arabidopsis* hypocotyls, the final microtubule orientation of fully grown cells is longitudinal (Crowell et al., 2009). Microtubule orientation in nongrowing trichomes was determined for agar-grown seedlings 18 d after germination. At this stage, cellulose synthesis had created thick secondary cell walls that prevented turgor-driven cell elongation (Supplemental Figures 3E and 3F). Both the GFP-TUB6 marker and the EB1-GFP marker indicated that microtubule density was reduced at this stage. However, we found longitudinal, helical, as well as a few transverse arrays in wild-type trichomes (the chosen example is right-handed) and mainly left-handed helical arrays in *tor2* (Supplemental Figures 3E and 3F). This suggests that in fully grown wild-type trichomes, and in contrast with hypocotyl epidermal cells, longitudinal microtubule orientation is not the default state.

### The *an1 dis1* Phenotype Is Additive

Trichomes of *tor2* are mildly overbranched, they are somewhat larger than the wild type, and, importantly, they show a right-handed twist in branches and stalks that develops during extension growth (Figures 3A and 3B) (Buschmann et al., 2009). Because the overall trichome phenotype of the α-tubulin mutant *tor2* is comparatively mild, it provides an ideal tool to analyze microtubule function by genetic means. Genetic screens have produced a wealth of information on factors involved in trichome branching and elongation. Some of these were implicated in microtubule-related processes. Among these are the *Arabidopsis* trichome mutants *an1* and *dis1* (Table 1, Figures 3C and 3D), which display defects in branching and elongation, respectively (Folkers et al., 2002; Le et al., 2003). To gain insight into the genetic pathways involving microtubules, we created the three respective double mutant combinations and analyzed the resultant trichome phenotypes.

Scanning electron microscopy revealed that the trichome phenotype of the *an1 dis1* double mutant is additive (Figure 3E). The trichomes showed mainly two branches and at the same time exhibited the typical *distorted* shape, i.e., at least one branch retained the capacity for extensive elongation, but it frequently showed swellings and alterations in the direction of growth. As such, the additive phenotype of *an1 dis1* double mutants indicates that there is no genetic interaction between the loci. This suggests that AN1-mediated trichome branching is independent of actin functions.

### The *an1 tor2* Double Mutant Shows an Unexpected Trichome Phenotype

We next isolated *an1 tor2* mutants. The *an1* single mutant showed weak left-handed petiole twisting; however, the double

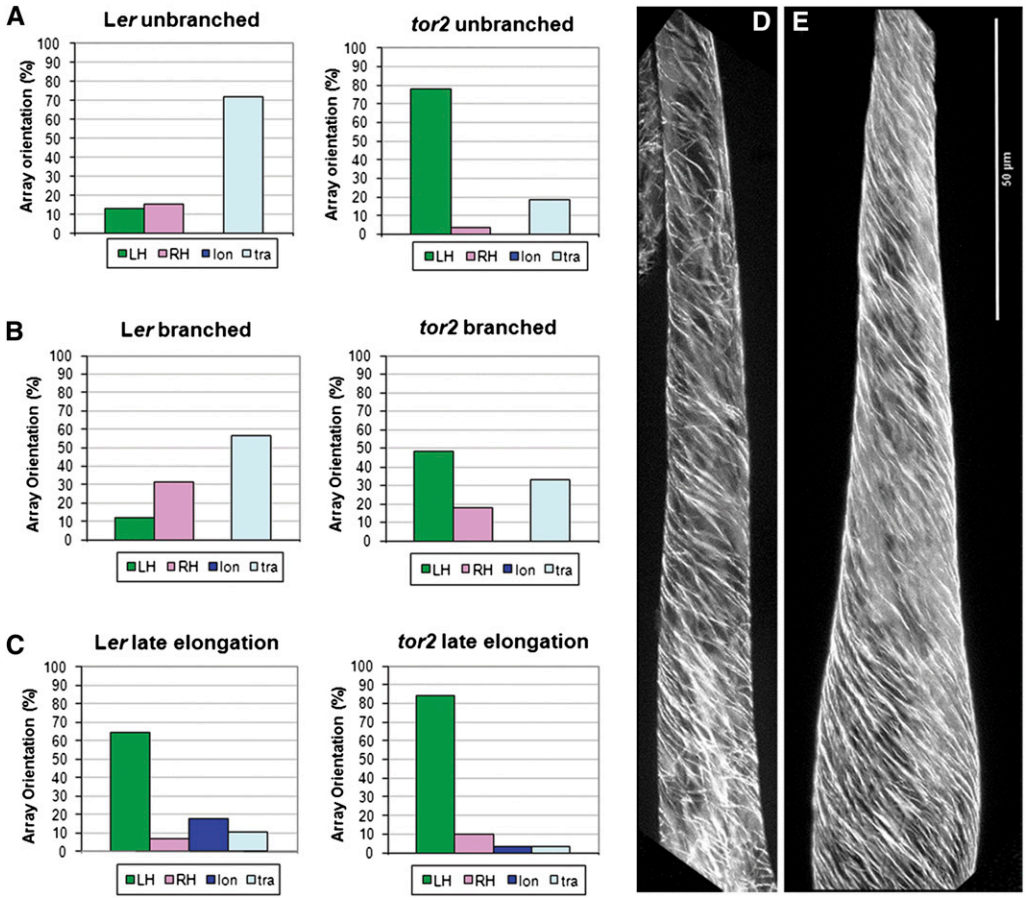


**Figure 2.** Handed Microtubule Arrays in Expanding Trichomes of L*er* Wild Type and *tor2*.

**(A)** Microtubule orientation in unbranched trichomes. Data of this stage were originally published in Buschmann et al. (2009).
**(B)** Microtubules in young branches smaller than 75 μm (L*er*, *n* = 60; *tor2*, *n* = 33).
**(C)** Microtubules in branches at late stages of growth (i.e., >75 μm) (L*er*, *n* = 28; *tor2*, *n* = 31). These quantitative assessments of microtubule alignment were based on EB1-GFP as a marker and t/z projected movies.
**(D)** Left-handed helical array seen in a late elongating wild-type branch (i.e., in a trichome branch >75 μm using GFP-TUB6).
**(E)** Left-handed array seen in late elongating *tor2* branch >75 μm using GFP-TUB6 (*n* = 66 and 62, respectively). Bar = 50 μm.
LH, left-handed; RH, right-handed; lon, longitudinal; tra, transverse.

homozygous *an1 tor2* double mutant showed right-handed petiole torsions similar to the *tor2* single mutant (Supplemental Figure 4A). Interestingly, in *an1 tor2* double mutants, many trichomes failed to initiate branches altogether (Figures 4A to 4D; Supplemental Figures 4A to 4C). Quantification showed that the double mutant is underbranched, even when compared with the *an1* single mutant (Figure 4D). The spike-like trichomes of *an1 tor2* retained the capacity to form a right-handed torque (using the cuticular papillae as landmarks; Figure 4C), but the single branch remained straight and did not show the *tor2*-typical swirl (compared with Figure 3B). The results showed that the overbranched *tor2* trichome mutant cannot complement underbranched *an1*. Instead, the *tor2*-induced microtubule defect enhanced the *an1* trichome phenotype. The results therefore suggest a synthetic genetic interaction between *tor2* and *an1*, and we propose that *an1* is hypersensitive to alterations in microtubule dynamics. To provide independent support for this genetic interaction we generated the double mutant of *an1* with the right-handed microtubule mutant *spiral1* (*spr1*) (Furutani et al., 2000). The results showed that *spr1* is epistatic to *an1* (in respect to petiole twisting), supporting the idea of a genetic interaction (Supplemental Figures 4D to 4F).

### Loss of Cell Anisotropy in *dis1 tor2* Double Mutants

The third double mutant pair, *dis1 tor2*, served to analyze the functional relationship of the two principal cytoskeletal systems of plants, microtubules, and actin filaments, in the anisotropy of trichome growth (Figure 5). *dis1* mutant trichomes have been reported to be "twisted" in appearance (Hülskamp et al., 1994; Le et al., 2003). We therefore first compared the twisting phenotype of *dis1* with *tor2*. Interestingly, we found that the direction of trichome twisting in *dis1* was not random. When viewed from above using the dissecting microscope (for

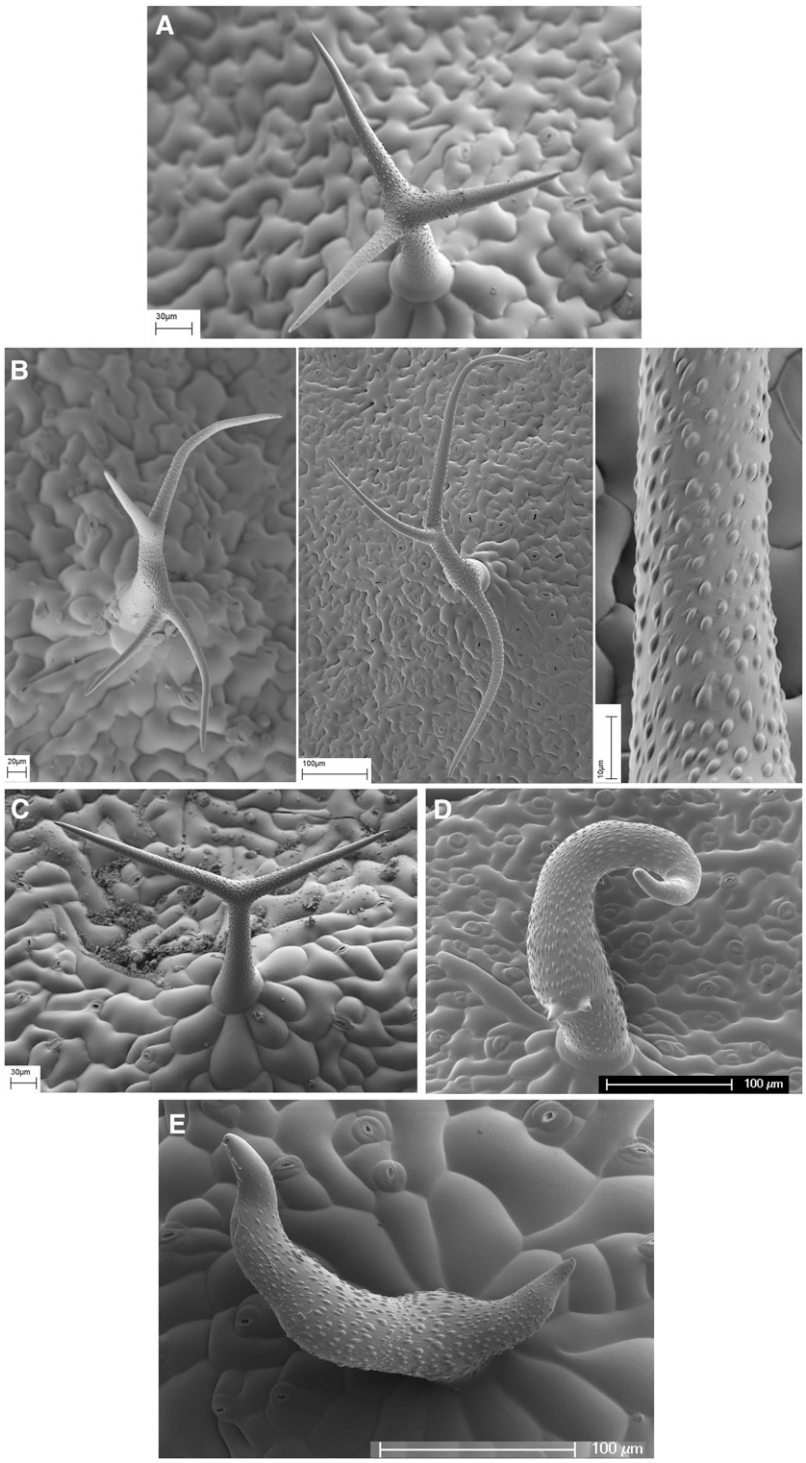


**Figure 3.** Phenotype of Trichome Mutants Used in This Study and the Additive Trichome Phenotype of *an1 dis1* Double Homozygous Plants as Observed by Scanning Electron Microscopy.

**(A)** L*er* wild type.
**(B)** *tor2* trichomes with four or three branches. Close-up of *tor2* branch showing a right-handed rotation of cuticular papillae.
**(C)** Underbranched *an1* trichome with two tips.
**(D)** Twisted appearance of *dis1* mutant trichome. Note the presence of three branch tips.
**(E)** Additive phenotype of *an1 dis1* mutant trichome.
Bars = 30 μm in **(A)**, 20, 100 and 10 μm in **(B)**, 30 μm in **(C)**, 100 μm in **(D)**, and 100 μm in **(E)**.

**Table 1.** Mutants Used for Double Mutant Analyses in This Study

| Mutant | Trichome Phenotype | Mutation Type | AGI No. | Protein Encoded by Wild-Type Gene | Assumed Wild-Type Protein Function |
|---|---|---|---|---|---|
| *tor2* | Overbranched and twisted | Dominant-negative | At1g04820 | α-Tubulin 4 | Microtubule subunit |
| *an1* (NASC3400) | Underbranched | Recessive | At1g01510 | CtBP/BARS | Golgi-related membrane traffic |
| *an1* (Salk026489) | Underbranched | Recessive, knockout | At1g01510 | CtBP/BARS | Golgi-related membrane traffic |
| *dis1-1* | Distorted (twisted) | Recessive, knockout | At1g13180 | ARP3 | ARP2/3 subunit, actin nucleation |
| *spr1* | n.a. | Recessive, knockout | At2g03680 | Microtubule-localized protein | Microtubule orientation |

AGI, Arabidopsis Genome Initiative; n.a., not analyzed.

quantification) or the electron microscope (Figure 5A), *dis1* trichomes were found to twist primarily to the right. We found 41.8% to be right-handed, 4.4% to be left-handed, and 25.8% to be straight ($n = 318$). In contrast with *tor2* (Buschmann et al., 2009), a relatively large number of *dis1* trichomes (28.0%) could not be assigned a specific handedness of twisting. Nonetheless, the quantification shows a clear bias toward right-handed twisting. Next, we aimed to establish whether this handedness defect in *dis1* trichomes was based on true cell twisting or rather on cell bending. Twisting implies that cell surface landmarks rotate along the cell's axis (i.e., that the cell shows a torque). In *tor2* trichomes, this rotation can be seen using the cuticular papillae as landmarks (Figure 3B). Bending (including staggered bends) would not show an obvious rotation of landmarks. We were unable to detect a clear direction of rotation for the cuticular papillae of *dis1* mutant trichomes (Supplemental Figure 5). This either means that the torque in *dis1* is based on cell bending rather than twisting or that the *dis1* phenotype is too weak to be detected by this method.

When *dis1* and *tor2* mutations were combined, a striking synthetic enhancement phenotype became apparent in the double homozygous plants (Figures 5B and 5D). The trichomes remained small and the overall appearance was one of a sphere. Although several normal branch initiation points were seen on every trichome, the branches themselves failed to elongate. Instead, the trichome trunk showed strong expansion, but fully or nearly isotropically. In the *dis1 tor2* combination, the cuticular papillae were frequently arranged in a helical manner encircling the trichome tip. In such cases, the helix was always right-handed. This indicates that DIS1 function is not required for expression of the *tor2*-induced twisted phenotype. The extreme bloated phenotype of *tor2 dis1* double mutant trichomes indicates a severe loss of growth anisotropy. As the phenotype is much more extreme (more than additive) when compared with the respective single mutants (compared with Figures 3B and 3D), it may be inferred that actin and microtubule functions buffer each other during diffuse growth. The cuticular papillae on the surface of *tor2 dis1* trichomes are a patchwork of both normal-looking and dramatically stretched papillae (Figure 5D), indicating that growth is no longer evenly distributed over the trichome's surface but becomes locally activated or restricted. This tends to suggest that actin and microtubule interactions are required for locally balancing growth activity.

### Defective Microtubule Reorganization in Developing *tor2 dis1* Trichomes

Next, we searched for any cytoskeletal defects underlying the enhanced cell shape defect of *tor2 dis1* trichomes. Microtubules were investigated first, using the GFP-TUB6 marker, and we focused on the cell elongation stage directly following branching. Wild-type and single mutant microtubules were imaged for comparison. In wild-type trichomes, a gradient of cortical microtubule density was observed increasing toward the branch tips (similar to what was already shown with the EB1-GFP marker; Supplemental Figure 2). These microtubules were mainly transverse (Figure 6A). Only few cortical microtubules were seen in the stalk. A similar distribution of microtubules was seen in *tor2*, that is, polymer concentration was highest at the branch tip. In general, *tor2* microtubules were well ordered (possibly even better than wild-type) and the microtubules assumed left-handed orientations (Figure 6B). When compared with the wild type, microtubules of *dis1* single mutants did not produce a comparable density gradient. Instead, microtubules were of similar density in the branches compared with the stalk. In some cases, microtubules of *dis1* mutant trichomes became slightly disordered (Figure 6C). In comparison to the single mutants, the trichomes of *tor2 dis1* plants showed a number of specific microtubule defects. Because these appeared to depend on the exact developmental stage, a developmental sequence, from the unbranched stage to early branch elongation, is presented (Figure 6D). Branching itself appeared normal and, as seen in the wild type, does not involve dense microtubule configurations at the branch site (asterisk on the first panel in Figure 6D). However, the produced tips had a strong tendency to become devoid of microtubules. This feature was visible throughout the whole developmental sequence (all panels in Figure 6D, arrowheads). Instead, microtubules concentrated in the trichome's stalk. Thus, when compared with the wild type, *tor2 dis1* trichomes showed an inverted gradient of microtubule density. Surprisingly, the microtubules of the stalk were well ordered even after cellular bloating had started (Figure 6D; Supplemental Figure 6A). Only at later expansion stages was it seen that *tor2 dis1* microtubules became disordered. Excessive ectopic accumulations of microtubules were seen at this stage (Figure 6D, arrows).

### Aberrant F-Actin in Growing Mutant Trichomes

Next, we performed the reciprocal experiment and explored the effects of *tor2 dis1* on F-actin organization in early elongating

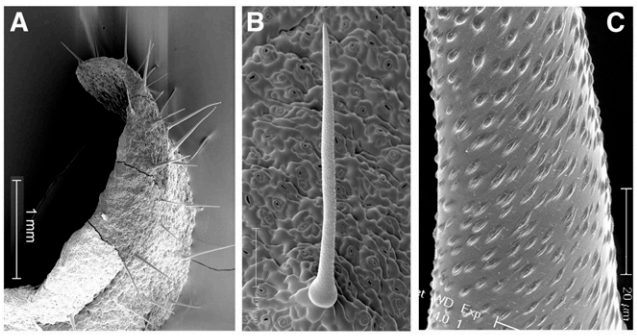


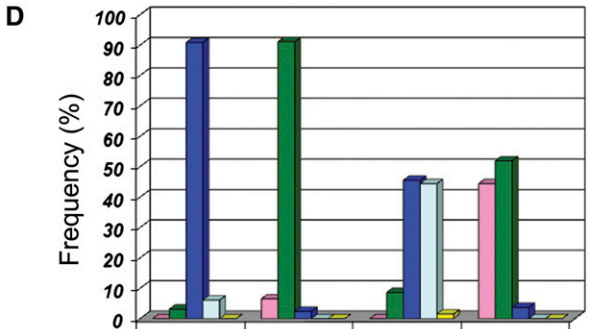


| | Ler | an1 | tor2 | an1 tor2 |
|---|---|---|---|---|
| 0 branch points | 0 | 6.5 | 0 | 44.4 |
| 1 branch point | 3.1 | 91.1 | 8.6 | 51.9 |
| 2 branch points | 90.8 | 2.4 | 45.5 | 3.7 |
| 3 branch points | 6.1 | 0 | 44.4 | 0 |
| 4 branch points | 0 | 0 | 1.5 | 0 |

**Figure 4.** The Underbranched Phenotype of *an1 tor2* Trichomes Indicates a Synthetic Genetic Interaction.

**(A)** Overview of an *an1 tor2* mutant leaf.
**(B)** Straight and unbranched trichome seen in *an1 tor2* background.
**(C)** Close-up of an *an1 tor2* trichome revealing that the cuticular papillae are arranged in a strictly right-handed manner.
**(D)** Frequency (%) of indicated branch point number as quantified for L*er* wild type, *an1*, *tor2*, and *an1 tor2* mutant background. The quantification was performed on trichomes seen on the first pair of true leaves.
Bars = 1 mm in **(A)**, 100 μm in **(B)**, and 20 μm in **(C)**.

trichomes. The respective single mutant lines and the wild type were used for comparison (Figures 7A to 7D). The experiments were based on the GFP-fABD2 marker line (Sheahan et al., 2004). The line was crossed with our mutants, and in the F2 generation, mutants and double mutants carrying the marker gene were selected and their offspring analyzed. Analyses confirmed and extended the results previously obtained for F-actin organization of the wild type (Mathur et al., 1999; Szymanski et al., 1999; Le et al., 2003). In the wild type, cables of F-actin radiating from the nucleus ascended into the growing branches (Figure 7A). These longitudinal cables were usually very straight and long, up to several tens of micrometers in length, and were mainly endoplasmic. These F-actin strands normally terminated before the actual tip, and, here, they frequently fused with the cell's cortex. Early elongating tips showed an additional feature. The cortical region of the wild-type branch tip was typically populated with a cap consisting of a fine mesh of F-actin (subsequently termed F-actin cap; brackets in Figure 7A). In its proximal position, the F-actin cap was frequently observed to overlap with the position of the microtubule collar seen at this stage (Figure 7A; Supplemental Figure 2C). The F-actin organization of *tor2* was generally quite similar to the wild type. However, we noticed that F-actin tended to be slightly bundled in *tor2*. This can be demonstrated by comparing the cortical F-actin network of *tor2* with the wild type or with the other mutants (see the cortical cytoskeleton in inset of Figure 7B and in Supplemental Figures 6B to

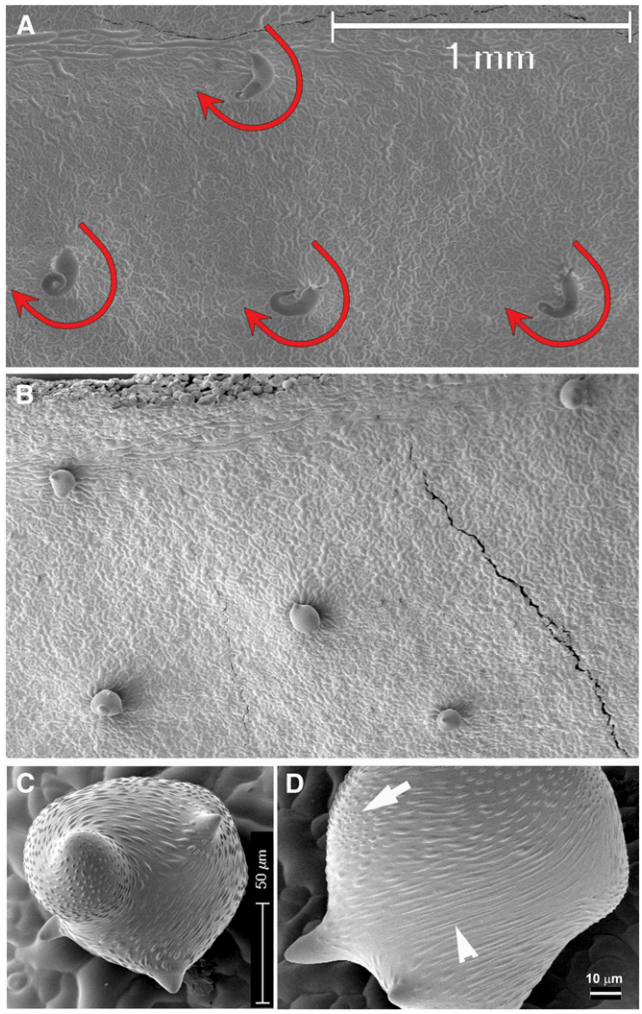


**Figure 5.** Phenotype of Trichomes Seen in *dis1* and *dis1 tor2* Double Mutants.

**(A)** *dis1* trichomes. Note the right-handed twist.
**(B)** *dis1 tor2* trichomes at the same magnification. The trichomes fail to develop a main axis and remain small.
**(C)** Although the *dis1 tor2* trichome shows a nearly complete loss of anisotropy, the *tor2*-specific torque is still visible. Branches are initiated but do not grow out.
**(D)** Close-up of a *dis1 tor2* trichome showing nearly normal (arrow) and dramatically stretched cuticular papillae (arrowhead).
Bars = 1 mm in **(A)** and **(B)**, 50 μm in **(C)**, and 10 μm in **(D)**.

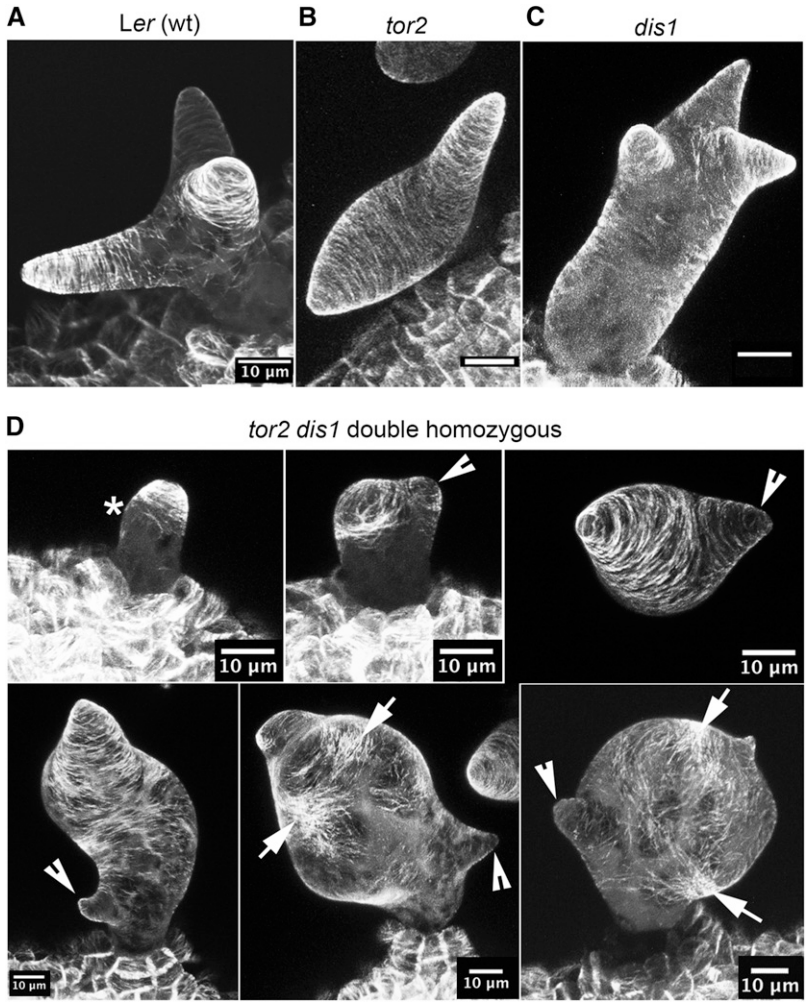


**Figure 6.** Microtubule Organization in Expanding *tor2 dis1* Double and Respective Single Mutants.

GFP-TUB6 was used to label microtubules in growing trichomes shortly after branching. Bars = 10 µm.
**(A)** L*er* wild-type trichome with transverse microtubule arrays. A gradient of microtubule density was observed with strongest signals in the tips.
**(B)** *tor2* mutant with a left-handed array.
**(C)** *dis1* mutant lacking a microtubule density gradient.
**(D)** Stages of trichome development in *tor2 dis1* double mutants (view from top-left to bottom-right). Initiation of the first branch in a *tor2 dis1* trichome (asterisk). In *tor2 dis1* double mutants, microtubules localized less efficiently to branch tips (arrowheads). Organized cortical microtubule arrays were seen only in the early stages soon after branching. Soon after, the arrays became more disorganized and striking patches of enhanced microtubule density were distributed on the now spherical trunk (arrows).

6E). The trichomes of *dis1* at this developmental stage showed an obvious defect concerning the organization of longitudinal actin cables. In agreement with earlier work (Le et al., 2003), the cables were shorter and were less efficiently targeted to the branch tips (Figure 7C). *tor2 dis1* trichomes were characterized by cytoplasmic actin cables that were even shorter and less well organized than in *dis1* (Figure 7D). In *tor2 dis1*, F-actin connecting the branch tips with the nucleus (or any other central location in the cell) was only rarely found. In fact, branch tips were frequently totally devoid of longitudinal F-actin cables (Figure 7D).

As stated above, when using the GFP-fABD2 marker line, trichomes of the wild type frequently showed a cap of fine F-actin in the tips of early elongating branches. We characterized the F-actin cap of wild-type trichomes by heat map analyses. In the example shown (Figure 7E), it can be seen that endoplasmic actin bundles (red) reach into the new tip (on right). The F-actin cap is identified by the strong signal (green-yellow) that is occupying the tip. Other cortical regions of the trichome have weaker signal. The intensity plot (from asterisk to asterisk) further demonstrates the elevated abundance of F-actin in the cap. The F-actin cap is also clearly seen in rotated 3D projections of wild-type trichomes expressing GFP-fABD2 (Supplemental Movie 4). Based on these features, we quantified the frequency with which branched trichomes of the early elongating stage showed an

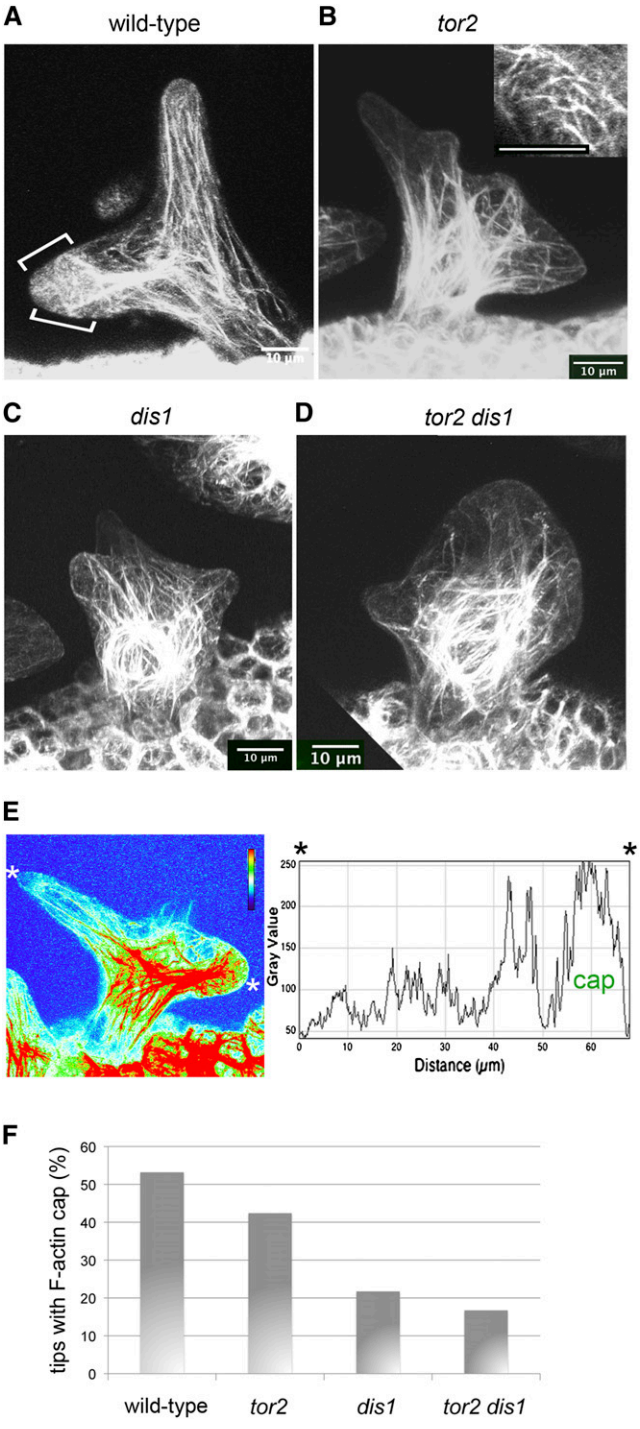


**Figure 7.** F-Actin Organization in Expanding *tor2 dis1* Double and Respective Single Mutants.

All analyses focused on early elongation growth just after branching using the GFP-fABD2 marker. Bars = 10 µm.

**(A)** In wild-type trichomes, F-actin density was strongest near the nucleus. From here, extended cables of F-actin were seen to run into the branches until they reach a region near the branch tip where they may fuse with the cell cortex. However, some cables run along the cortex. In addition, the early extending trichome tip presents a mesh of fine cortical F-actin (brackets in **[A]** indicate the F-actin cap).

**(B)** The overall F-actin organization in *tor2* trichomes at this stage is similar to the wild type. However, it was noticed that *tor2* trichomes showed prominent F-actin filaments or bundles at the cell cortex (see projection of cortical z-levels in inset).

**(C)** *dis1* mutant trichomes showed the typical defects of *dis* class mutants described previously. The longitudinal F-actin cables appeared short and less clearly directed toward the trichome tips. In addition, a cap of F-actin was rarely seen in *dis1* tips.

**(D)** In *tor2 dis1* double mutant trichomes, F-actin organization is clearly aberrant. The nucleus is typically caged by a striking accumulation of actin. Longitudinal F-actin cables extending into the cytoplasm are rare. F-actin cables are very short and directed in apparently random directions. Trichome tips appear empty and are almost never connected with nuclear actin cables.

**(E)** Characterization of the F-actin cap seen in early elongating wild-type trichome expressing GFP-fABD2 by heat map analysis and corresponding intensity profile. A line drawn between the asterisks (shown in the heat map) was used to calculate the intensity plot.

**(F)** Frequency with which the F-actin cap was observed in the tips of wild-type and mutant trichome branches.

F-actin cap. We found that 53.2% of wild-type branch tips exhibited an obvious F-actin cap (Figure 7F; $n$ = 79). Next, we investigated whether the F-actin cap was formed with normal frequency in the *dis1* and *tor2* derived lines (Figure 7F). Whereas in *tor2* the frequency with which the F-actin cap could be observed was only slightly diminished (42.4%; $n$ = 66), a strong reduction in frequency was found in *dis1* (21.7%; $n$ = 60) and in *tor2 dis1* (16.7%; $n$ = 48).

## DISCUSSION

### Marking the Branch Point

Molecular-genetic and pharmacological studies have established that microtubules are essential for branch initiation in *Arabidopsis* (Mathur and Chua, 2000; Smith and Oppenheimer, 2005; Szymanski, 2009). This function was previously assigned to cortical microtubules that accumulate in a collar at the apical part of the unbranched trichome (Folkers et al., 2002; Beilstein and Szymanski, 2004). In this investigation, we further characterized this collar by labeling microtubules in living trichome cells before and during branching. Building on earlier work (Mathur and Chua, 2000; Beilstein and Szymanski, 2004), we aimed at increasing the resolution of the developmental sequence leading to trichome branching and to determine how cortical microtubules colonize the new branch (Figure 1). For this, we employed GFP-TUB6 and EB1-GFP markers. The analyses showed that the new branch was always formed underneath the apical microtubule collar in a region of reduced microtubule density. The few remaining microtubules in the region of the incipient bulge were rather random in their organization. This suggested that the bulging itself does not depend on microtubules. The situation is reminiscent of root hair emergence in lettuce (*Lactuca sativa*), where microtubules become disorganized in the region of the bulge. Moreover, under certain conditions,

microtubule-depolymerizing oryzalin can induce root hair formation (Takahashi et al., 2003).

Our finding that an apical microtubule collar is involved in trichome branching yet the bulge occurs beneath the collar in an area of reduced microtubule density can be explained if the microtubule collar marks the area for bulge formation but becomes progressively separated from it by continued growth of the trichome apex (see model in Figure 8A). Trichomes are known to elongate by diffuse growth (Schwab et al., 2003); however, the same study also showed that trichome branches grow faster at their tips. That *Arabidopsis* trichomes may combine tip growth with elongation growth was suggested previously (Szymanski et al., 1999; Beilstein and Szymanski, 2004). If we assume that the unbranched trichome grows by tip growth, a scenario emerges in which microtubules function in marking the branch point, but as bulging occurs somewhat later (after the microtubule collar has moved on), microtubules need not to be present when the bulge grows out. Accordingly, the microtubule collar could function in delivering proteins to the "bulge to come." It is too early to pinpoint which proteins are involved (yellow cloud in model of Figure 8A), but proteins such as BRANCHLESS TRICHOME and STICHEL, which have been seen to accumulate at the tip of early trichome branches (Ilgenfritz et al., 2003; Marks et al., 2009), are potential candidates.

### The Branch Number Is Regulated by Microtubule Dynamics and Golgi Functions

As published earlier, *tor2* mutants are overbranched (Buschmann et al., 2009), and we therefore investigated the microtubule configurations of *tor2* during branching. We frequently observed ectopic accumulations of cortical microtubules in trichomes undergoing branch initiation (Figure 1F). It is conceivable that altered microtubule dynamics of the *tor2* background led to local stabilization of microtubules (leading to bundling) and that these ectopic microtubules induced additional branch sites. Testing microtubule function during branching by introgressing the *an1* mutation into *tor2* resulted in a surprising phenotype (Figure 4). The *an1 tor2* double mutant is underbranched even in comparison to the already underbranched *an1* mutant. The phenotype suggests that AN1 function and normal microtubule dynamics can buffer each other. It also means that in *tor2*, branching is heavily dependent on AN1 function and that *an1* mutants are hypersensitive to alterations in microtubule dynamics (i.e., stabilization). AN1 is a CtBP/BARS protein implicated in the trafficking of Golgi membranes (Folkers et al., 2002; Kim et al., 2002). A function for microtubule stability in trichome branching was suggested by earlier work (Mathur and Chua, 2000), and our results support the idea that fine-tuning microtubule dynamics is important for a Golgi-based mechanism of trichome branching. A connection between Golgi and microtubules was also suggested by analysis of Kinesin-13A of *Arabidopsis* (Lu et al., 2005). This kinesin is assumed to function in the distribution of Golgi stacks and its knockout mutant may be mildly overbranched. Considered together with our results, it appears that both microtubule dynamics and Golgi activity need to be finely balanced to produce a normal branching pattern.

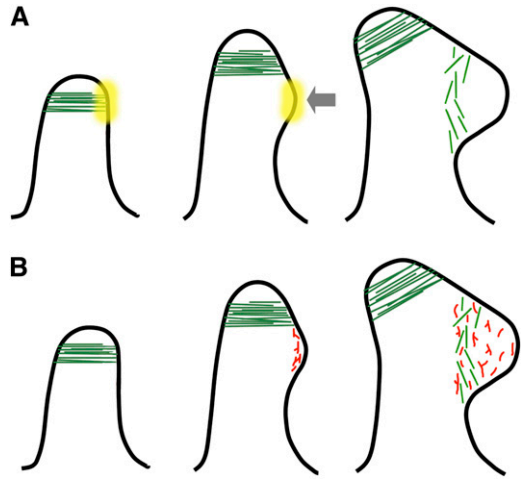


**Figure 8.** Model for Cortical Microtubule and Actin Function in Trichome Branching.

**(A)** We hypothesize that the unbranched trichome elongates mainly by tip growth. The microtubule collar (green) marks the branch site. The primary tip keeps on elongating but the mark (depicted by the yellow cloud) remains at the exact cortical position. The bulge then forms at the mark. Microtubules are not present at this stage, nor do they seem to be required, but shortly after, the new microtubule collar is formed at the base of the secondary tip.

**(B)** For clarity, only the F-actin network at the new branch site is shown. F-actin (in red, branched) is present at the center of the new bulge before microtubules (in green) colonize the nascent branch. F-actin is involved in preparing the cortex in a manner that enables cortical microtubules to eventually occupy the same position.

### As the Bulge Becomes a Branch

It was previously shown that the microtubules on the new branch arrange in a fashion very similar to the microtubule collar of the unbranched trichome (Folkers et al., 2002; Beilstein and Szymanski, 2004). In this study we aimed to clarify how this secondary collar is formed in the wild type. Our results suggest that the new collar is not derived from cortical microtubules of the primary collar, but is assembled de novo. The nascent secondary collar is faint and wide (up to 10 μm) in the beginning, but soon becomes stronger and eventually narrows as the branch enlarges.

Pharmacological experiments and mutant analysis suggest that the actin cytoskeleton is not involved in branch initiation; however, normal branch expansion is still dependent on F-actin. We therefore localized F-actin in young branching trichomes of the wild type using the GFP-fABD2 marker. We found that at the earliest sign of branching, a faint signal outlined the swelling bulge, indicating that F-actin localized to this site (Figures 1I and 1J). This signal became stronger until an F-actin cap was seen to label the distal end of the young branch (Figure 1L). This process of F-actin cap formation is apparently iterated in the later branching events (Figure 7). Therefore, the situation is similar to tip-growing cells like root hairs and pollen tubes where a cap of F-actin was frequently found near the growth apex (Gibbon et al., 1999; Baluska et al., 2000; Hepler et al., 2001;

Samaj et al., 2006). Cortical F-actin in growing trichome tips has been observed previously (Szymanski et al., 1999; Le et al., 2003; Szymanski, 2009); however, the structure of an F-actin cap appears to be especially clear when using the GFP-fABD2 marker (Jörgens et al., 2010). That the GFP-fABD2 marker is particularly useful for observing fine and dynamic F-actin in living cells was shown previously (Staiger et al., 2009). Our finding of an F-actin cap in young branches also supports the idea that at an early stage, trichome branches grow by tip growth (Hepler et al., 2001; Beilstein and Szymanski, 2004; Tominaga-Wada et al., 2011). Furthermore, if F-actin is compared with cortical microtubule localization during trichome bulging, it becomes clear that actin localizes to the new branch tip before microtubules do. It is tempting to speculate that actin functions in attracting microtubules to the growing branch tip (also see model in Figure 8B). Some evidence for this is presented by the *dis1* single and *tor2 dis1* double mutants (see below).

### The *tor2 dis1* Phenotype Indicates a Genetic Interaction of Actin and Microtubules

Based on the dramatically swollen phenotype of the *dis1 tor2* double mutant, we conclude that both cytoskeletal systems, microtubules, and F-actin must interact to facilitate normal plant cell expansion. The double mutant phenotype was not anticipated from inspecting the individual mutants, and it is therefore suggested that the phenotype is caused by a synthetic genetic interaction. Despite the double mutant's dramatic loss of anisotropy, these spherical cells show correctly initiated branch points. This shows that the interaction of the two cytoskeletal systems is specifically required for normal cell expansion, in contrast with trichome branch initiation, where interfering with F-actin has little impact (Szymanski et al., 1999).

The analysis of microtubules in *dis1* and *tor2 dis1* mutants produced additional insight into the regulation of growth anisotropy in trichomes (Figure 6). It appears that actin is required to enable the microtubules to produce a gradient with microtubule density being strongest at the branch tip. This is suggested by the microtubule phenotype of *dis1* mutants. In *tor2 dis1* mutants, this is even more obvious, where microtubules are absent from the branch tip altogether. This suggests that actin is required to enable microtubules to populate the tip, especially when microtubules are stabilized by the *tor2* mutation. It is possible that tip- localized F-actin enables or prepares the cortex to sequester microtubules. This possibility is also indicated by our analysis of microtubule and actin localization during the first branching events (Figure 1). In that case, F-actin is found in the bulge first and is then followed by microtubules. In addition, the trunk of *tor2 dis1* trichomes showed extensive isotropic swelling, indicating that cortical microtubules were dysfunctional (Figure 6D). The microtubule phenotype of the early stages of *tor2 dis1* expansion growth resembled a taxol-like effect in that cortical microtubules were present and well ordered but apparently unable to determine the direction of growth (Supplemental Figure 6A). This could mean that actin supports microtubule dynamics, at least in *tor2*. *tor2* is known to have stabilized microtubules in trichomes (Buschmann et al., 2009) and it appears that the *dis1* mutation exaggerates the effect, with concomitant effects on cell wall synthesis. This is reasonable, since it was suggested previously that the linking of cellulose synthase complexes to cortical microtubules may be dependent on dynamic microtubules (Chan et al., 2010). In summary, the *tor2 dis1* double mutant has two specific microtubule defects: (1) the branches do not get colonized by cortical microtubules (this may be considered a reorientation defect) and (2) the cortical microtubules of the trunk are incapable of supporting anisotropic cell growth (which appears to result from enhanced microtubule stabilization).

During the course of our experiments with the GFP-fABD2 marker, we realized that a cap of F-actin frequently occurs in the early elongating tips of wild-type trichomes (Figures 1L, 7A, and 7E; Supplemental Movie 4). In our data set, 53.2% of the elongating wild-type trichome tips showed this feature. We expect that this value will increase once the developmental stage for its occurrence (i.e., the exact tip size) is better characterized. It seems likely that the F-actin cap is seen as long as tip growth dominates; once elongation growth takes over the cap might disappear. However, our quantification showed that the F-actin cap is often missing in *dis1* mutants and to an even greater extent in the *tor2 dis1* double mutants (Figure 7F). In this regard, it is interesting that in the wild type the nascent branch tip is colonized by F-actin before microtubules arrive (Figure 1). It is possible that the F-actin cap is important for organizing microtubules, as the *dis1* and *tor2 dis1* mutants also show defects in microtubule reorientation (as discussed above). Accordingly, the lack of the F-actin cap in *dis1* and *tor2 dis1* mutants may make it impossible for microtubules to colonize the branch tips and to form the typical tip-directed gradient of microtubule density seen in the wild type (Figure 6A). The lack of cortical microtubules in the tips, in turn, may contribute to stalling branch elongation.

In algae and land plants, there is accumulating evidence that actin networks interact with microtubules (reviewed in Collings, 2008). Cooperation of microtubules with actin was suggested for the trafficking of cellulase synthase complexes during vessel formation (Wightman and Turner, 2008). Moreover, colocalization and interdependent behavior of actin and microtubules was reported for the *Arabidopsis* hypocotyl (Sampathkumar et al., 2011). That there might be an interaction between actin and microtubules in the diffuse growth of trichomes was suggested by analyzing GFP-tagged microtubule markers in *dis* mutants where microtubules were repeatedly found to be ill-aligned in mature trichomes (Schwab et al., 2003; Saedler et al., 2004; Zhang et al., 2005). Recently, the localization of the ARP2/3 complex in *Arabidopsis* pavement cells showed that a subpool of the complex localizes to cortical microtubules (Zhang et al., 2013). In this regard, it may be relevant that a potential subunit of the SCAR/WAVE complex involved in ARP2/3 activation, ABIL3, was shown to bind to plant microtubules upon overexpression (Jörgens et al., 2010). In addition, some plant proteins are known for binding both filament types directly (Petrásek and Schwarzerová, 2009), including a group of recently characterized kinesins (Xu et al., 2009; Buschmann et al., 2011; Klotz and Nick, 2012). While these articles present important indirect and direct evidence for an interplay between microtubules and actin, our analysis provides direct support for a genetic interaction in plant cell growth: The phenotype of the *dis1 tor2* double mutant shows that actin and microtubule networks are

required to cooperate in trichome expansion growth and that in single mutants of either system, growth anisotropy is at least partially buffered by the other.

### A Hidden Handedness in *Arabidopsis* Trichomes

Helical growth in *Arabidopsis* was originally considered a phenomenon expressed only by whole organs (Furutani et al., 2000), but the *tor2* phenotype and theoretical models suggest that in at least some helical growth mutants, the actual basis of helical growth may be the single cell (Schulgasser and Witztum, 2004; Buschmann et al., 2009; Eren et al., 2010; Wada, 2012). In this article, we show that even growing wild-type *Arabidopsis* trichome cells show helical microtubule arrays of consistent handedness (Figure 2C). This microtubule phenotype is seen in late-elongating (presumably decelerating) trichomes. Similarly, although expressed in tissues, cortical microtubules of *Arabidopsis* and maize roots adopt helical configurations of specific handedness during late elongation (Liang et al., 1996; Sugimoto et al., 2000). Together, the results suggest that the impact of microtubule orientation on the direction of growth depends on the developmental stage, being strongest at an early stage. Our finding that the twisting of *dis1* trichomes shows a handedness bias (Figure 5A) supports the concept of an interaction between actin and microtubule networks. We speculate that the intrinsically asymmetric microtubule orientations of the wild type (Figure 2C) are normally buffered by actin functions and that this microtubule-based handedness becomes visible in the *dis1* background. Many plant cells when growing in isolation show some degree of handed twisting (Preston, 1974). Interestingly, there is twisting in cotton trichome growth from the earliest stages on, and the results presented by Stewart (1975) strongly suggest that there is a specific handedness to the process.

### Conclusion

Taken together, our cell biological and genetic data show that cortical microtubules have actin-dependent and actin-independent functions in the differentiation of *Arabidopsis* trichomes. The genetic analyses suggest that trichome branching requires the balancing of microtubule dynamics and Golgi functions; however, actin is not directly involved. By contrast, trichome cell expansion requires an interaction of actin and microtubule networks, as exemplified by the swollen *tor2 dis1* double mutant phenotype. The taxol-like effect on microtubules suggests that knocking out *dis1* leads to hyperstabilized microtubules in the *tor2* background. Furthermore, the actin cytoskeleton is required to allow microtubules to reorganize and to localize correctly to the tips of enlarging branches. The precise mechanism for an interaction between F-actin and microtubules in this process is unknown, but our data suggest that an F-actin cap in the tip of young trichome branches plays a part.

## METHODS

#### Mutant Strains and Marker Lines

*Arabidopsis thaliana* plants carrying the α-tubulin 4 R2K (*tor2*) mutation were described (Buschmann et al., 2009). *tor2* was crossed to *dis1-1* and *an1* mutants. The mutations *tor2*, *dis1-1*, and *an1* map to the top of chromosome 1, and considerable linkage of the loci was observed. However, double homozygous mutants were routinely identified in segregating F3 families. The *an1* (Landsberg *erecta* [L*er*] allele) and the *an1 dis1-1* double mutant were obtained from the Nottingham Arabidopsis Stock Centre (N3400 and N2, respectively). Seeds of the *dis1-1* mutant line were a kind gift of Karim Sorefan (University of East Anglia, Norwich). All mutants used in this study are in L*er* background, except *spr1* and *an1* (Salk 026489 allele), which are in Columbia-0 background. All marker lines used in this study are in L*er* background, except the GFP-fABD2 line, which is in Columbia-0 background. Marker lines expressing GFP-labeled microtubule markers were described by Buschmann et al. (2009). The GFP-fABD2 line was described by Sheahan et al. (2004).

#### Confocal Microscopy and Analysis of Image Data

GFP-based microscopy of trichomes was performed using the Visitech spinning disc confocal microscope or the Zeiss 510 Meta microscope. All microscopy was performed using a 60-fold immersion objective. For the investigation of microtubule dynamics and their alignment in trichomes, both mutant and marker plants were grown on Paul's agar (Buschmann et al., 2011) until analysis, which was 11 to 12 d after germination for elongating trichomes. Trichomes were selected from the 3rd to 6th true leaf. Trichome branches of the early (≤75 μm) and the late elongation (>75 μm) stage were measured and distinguished under the confocal microscope. In addition, to ensure that the trichomes with branches >75 μm were still elongating, they were compared with trichomes of older leaves of the same plant, which at this point in time were larger (Supplemental Figure 3). Nongrowing trichomes were identified in plants 18 d after germination. These trichomes showed cell walls with increased thickness. For live-cell microscopy, leaves were excised under the dissecting microscope using a diluted Murashige and Skoog solution as medium and placed in the live chamber. The live chamber uses a gas-permeable membrane for gas exchange during microscopy (Buschmann et al., 2010). Movies were assembled and analyzed with the aid of the ImageJ software (W. Rasband, NIH). ImageJ plug-ins also served to produce heat maps and 3D rotations. The quantification of microtubule orientation in growing trichomes was performed as described (Buschmann et al., 2009).

#### Scanning Electron Microscopy

Leaf samples (3rd to 5th true leaf) were mounted on an aluminum stub using O.C.T. compound (British Drug House Laboratory Supplies). The stub was then immediately plunged into liquid nitrogen slush to cryopreserve the material. The sample was transferred to the cryostage of an ALTO 2500 cryo-transfer system (Gatan) attached to a Zeiss Supra 55 VP FEG scanning electron microscope (Zeiss SMT). Sublimation of surface frost was performed at −95°C for 3 min before sputter-coating the sample with platinum for 2 min at 10 mA, at temperatures below −110°C. After sputter-coating, the sample was moved to the cryostage in the main chamber of the microscope, held at approximately −130°C. The sample was imaged at 3 kV, and digital TIFF files were stored.

#### Quantification of Trichome Branching

Branching was quantified using a Leica dissecting microscope with variable magnification assisted by an additional lateral light source (to enhance contrast) as described (Buschmann et al., 2009). As the *an1 tor2* branching phenotype appeared to be more pronounced on primary leaves (compared with later leaves), all quantifications (including L*er*, *tor2*, and *an1*) were done at this stage.

### Accession Numbers

The main mutants used in this investigation correspond to the following genes (accession numbers according to the Arabidopsis Genome Initiative): *AN1* (At1g01510), *DIS1* (At1g13180), *TOR2*/*TUA4* (At1g04820).

### Supplemental Data

The following materials are available in the online version of this article.

**Supplemental Figure 1.** The GFP-TUB6 Line Suggests That in Trichome Branching, the Formation of the Early Bulge Occurs without Cortical Microtubule Accumulations.

**Supplemental Figure 2.** EB1-GFP Visualizes a Wide Ring of Microtubules Formed on Early Bulging Trichome Branches.

**Supplemental Figure 3.** Assessment of Microtubule Orientation in Late-Growing and Fully Grown Trichomes Using Various Microtubule Markers.

**Supplemental Figure 4.** Details on *an1 tor2* and *an1 spr1* Double Mutants.

**Supplemental Figure 5.** Phenotype of *dis* Trichomes, as Revealed by Scanning Electron Microscopy.

**Supplemental Figure 6.** Additional Examples of an Aberrant Cytoskeleton in *tor2 dis1* and Respective Single Mutants.

**Supplemental Movie 1.** L*er* Wild-Type Trichome Expressing EB1-GFP before Branching.

**Supplemental Movie 2.** L*er* Wild-Type Trichome Expressing EB1-GFP at Early Branch Formation.

**Supplemental Movie 3.** *tor2* Trichome Expressing EB1-GFP at Branching.

**Supplemental Movie 4.** 3D Rotation of a Wild-Type Trichome Expressing GFP-fABD2.

## ACKNOWLEDGMENTS

We thank Porntip Green (John Innes Centre, Norwich) for help in maintaining *Arabidopsis* mutant lines. We also thank Sabine Zachgo (Botany Chair in Osnabrück) for hosting the final stages of this microtubule project. This work was supported by a Biotechnology and Biological Science Research Council program grant to C.W.L. and by a SFB944 (Deutsche Forschungsgemeinschaft) start-up grant to H.B.

## AUTHOR CONTRIBUTIONS

H.B., A.R.S., and C.W.L. designed the research. H.B., A.S., and K.F. performed the experiments. H.B., A.S., and C.W.L. analyzed the data. H.B. wrote the article. A.R.S. and C.W.L. contributed to writing.

Received September 13, 2013; revised February 14, 2014; accepted February 20, 2014; published April 8, 2014.

## REFERENCES

**Abe, T., Thitamadee, S., and Hashimoto, T.** (2004). Microtubule defects and cell morphogenesis in the *lefty1 lefty2* tubulin mutant of *Arabidopsis thaliana*. Plant Cell Physiol. **45:** 211–220.

**Bai, Y., Falk, S., Schnittger, A., Jakoby, M.J., and Hülskamp, M.** (2010). Tissue layer specific regulation of leaf length and width in Arabidopsis as revealed by the cell autonomous action of ANGUSTIFOLIA. Plant J. **61:** 191–199.

**Baluska, F., Salaj, J., Mathur, J., Braun, M., Jasper, F., Samaj, J., Chua, N.H., Barlow, P.W., and Volkmann, D.** (2000). Root hair formation: F-actin-dependent tip growth is initiated by local assembly of profilin-supported F-actin meshworks accumulated within expansin-enriched bulges. Dev. Biol. **227:** 618–632.

**Beilstein, M., and Szymanski, D.B.** (2004). Cytoskeletal requirements during Arabidopsis tichome development. In The Plant Cytoskeleton in Cell Differentiation and Development, P. Hussey, ed (Oxford, UK: Blackwell), pp. 265–289.

**Blanchoin, L., Amann, K.J., Higgs, H.N., Marchand, J.B., Kaiser, D.A., and Pollard, T.D.** (2000). Direct observation of dendritic actin filament networks nucleated by Arp2/3 complex and WASP/Scar proteins. Nature **404:** 1007–1011.

**Burk, D.H., Liu, B., Zhong, R., Morrison, W.H., and Ye, Z.H.** (2001). A katanin-like protein regulates normal cell wall biosynthesis and cell elongation. Plant Cell **13:** 807–827.

**Buschmann, H., and Lloyd, C.W.** (2008). *Arabidopsis* mutants and the network of microtubule-associated functions. Mol. Plant **1:** 888–898.

**Buschmann, H., Green, P., Sambade, A., Doonan, J.H., and Lloyd, C.W.** (2011). Cytoskeletal dynamics in interphase, mitosis and cytokinesis analysed through Agrobacterium-mediated transient transformation of tobacco BY-2 cells. New Phytol. **190:** 258–267.

**Buschmann, H., Hauptmann, M., Niessing, D., Lloyd, C.W., and Schäffner, A.R.** (2009). Helical growth of the *Arabidopsis* mutant *tortifolia2* does not depend on cell division patterns but involves handed twisting of isolated cells. Plant Cell **21:** 2090–2106.

**Buschmann, H., Sambade, A., Pesquet, E., Calder, G., and Lloyd, C.W.** (2010). Microtubule dynamics in plant cells. Methods Cell Biol. **97:** 373–400.

**Chan, J., Crowell, E., Eder, M., Calder, G., Bunnewell, S., Findlay, K., Vernhettes, S., Höfte, H., and Lloyd, C.** (2010). The rotation of cellulose synthase trajectories is microtubule dependent and influences the texture of epidermal cell walls in Arabidopsis hypocotyls. J. Cell Sci. **123:** 3490–3495.

**Collings, D.A.** (2008). Crossed-wires: Interactions and cross-talk between the microtubule and microfilament networks in plants. In Plant Microtubules Development and Flexibility, P. Nick, ed (Berlin-Heidelberg: Springer), pp. 47–79.

**Corda, D., Colanzi, A., and Luini, A.** (2006). The multiple activities of CtBP/BARS proteins: The Golgi view. Trends Cell Biol. **16:** 167–173.

**Crowell, E.F., Bischoff, V., Desprez, T., Rolland, A., Stierhof, Y.D., Schumacher, K., Gonneau, M., Höfte, H., and Vernhettes, S.** (2009). Pausing of Golgi bodies on microtubules regulates secretion of cellulose synthase complexes in *Arabidopsis*. Plant Cell **21:** 1141–1154.

**Eren, E.C., Dixit, R., and Gautam, N.** (2010). A three-dimensional computer simulation model reveals the mechanisms for self-organization of plant cortical microtubules into oblique arrays. Mol. Biol. Cell **21:** 2674–2684.

**Folkers, U., Kirik, V., Schöbinger, U., Falk, S., Krishnakumar, S., Pollock, M.A., Oppenheimer, D.G., Day, I., Reddy, A.S., Jürgens, G., and Hülskamp, M.** (2002). The cell morphogenesis gene ANGUSTIFOLIA encodes a CtBP/BARS-like protein and is involved in the control of the microtubule cytoskeleton. EMBO J. **21:** 1280–1288. Erratum. EMBO J. **21:** 2507.

**Furutani, I., Watanabe, Y., Prieto, R., Masukawa, M., Suzuki, K., Naoi, K., Thitamadee, S., Shikanai, T., and Hashimoto, T.** (2000).

The SPIRAL genes are required for directional control of cell elongation in *Arabidopsis thaliana*. Development **127:** 4443–4453.

**Gibbon, B.C., Kovar, D.R., and Staiger, C.J.** (1999). Latrunculin B has different effects on pollen germination and tube growth. Plant Cell **11:** 2349–2363.

**Hepler, P.K., Vidali, L., and Cheung, A.Y.** (2001). Polarized cell growth in higher plants. Annu. Rev. Cell Dev. Biol. **17:** 159–187.

**Hülskamp, M., Misŕa, S., and Jürgens, G.** (1994). Genetic dissection of trichome cell development in *Arabidopsis*. Cell **76:** 555–566.

**Ilgenfritz, H., Bouyer, D., Schnittger, A., Mathur, J., Kirik, V., Schwab, B., Chua, N.H., Jürgens, G., and Hülskamp, M.** (2003). The Arabidopsis STICHEL gene is a regulator of trichome branch number and encodes a novel protein. Plant Physiol. **131:** 643–655.

**Ishida, T., Kaneko, Y., Iwano, M., and Hashimoto, T.** (2007). Helical microtubule arrays in a collection of twisting tubulin mutants of *Arabidopsis thaliana*. Proc. Natl. Acad. Sci. USA **104:** 8544–8549.

**Jörgens, C.I., Grünewald, N., Hülskamp, M., and Uhrig, J.F.** (2010). A role for ABIL3 in plant cell morphogenesis. Plant J. **62:** 925–935.

**Kim, G.T., Shoda, K., Tsuge, T., Cho, K.H., Uchimiya, H., Yokoyama, R., Nishitani, K., and Tsukaya, H.** (2002). The ANGUSTIFOLIA gene of Arabidopsis, a plant CtBP gene, regulates leaf-cell expansion, the arrangement of cortical microtubules in leaf cells and expression of a gene involved in cell-wall formation. EMBO J. **21:** 1267–1279.

**Kirik, V., Grini, P.E., Mathur, J., Klinkhammer, I., Adler, K., Bechtold, N., Herzog, M., Bonneville, J.M., and Hülskamp, M.** (2002). The *Arabidopsis* TUBULIN-FOLDING COFACTOR A gene is involved in the control of the alpha/beta-tubulin monomer balance. Plant Cell **14:** 2265–2276.

**Klotz, J., and Nick, P.** (2012). A novel actin-microtubule cross-linking kinesin, NtKCH, functions in cell expansion and division. New Phytol. **193:** 576–589.

**Kotchoni, S.O., Zakharova, T., Mallery, E.L., Le, J., El-Assal, Sel.-D., and Szymanski, D.B.** (2009). The association of the Arabidopsis actin-related protein2/3 complex with cell membranes is linked to its assembly status but not its activation. Plant Physiol. **151:** 2095–2109.

**Le, J., El-Assal, Sel.-D., Basu, D., Saad, M.E., and Szymanski, D.B.** (2003). Requirements for Arabidopsis ATARP2 and ATARP3 during epidermal development. Curr. Biol. **13:** 1341–1347.

**Liang, B.M., Dennings, A.M., Sharp, R.E., and Baskin, T.I.** (1996). Consistent handedness of microtubule arrays in maize and *Arabidopsis* primary roots. Protoplasma **190:** 8–15.

**Lu, L., Lee, Y.R., Pan, R., Maloof, J.N., and Liu, B.** (2005). An internal motor kinesin is associated with the Golgi apparatus and plays a role in trichome morphogenesis in *Arabidopsis.* Mol. Biol. Cell **16:** 811–823.

**Maisch, J., Fiserová, J., Fischer, L., and Nick, P.** (2009). Tobacco Arp3 is localized to actin-nucleating sites *in vivo.* J. Exp. Bot. **60:** 603–614.

**Marks, M.D., Esch, J., Herman, P., Sivakumaran, S., and Oppenheimer, D.** (1991). A model for cell-type determination and differentiation in plants. Symp. Soc. Exp. Biol. **45:** 77–87.

**Marks, M.D., Wenger, J.P., Gilding, E., Jilk, R., and Dixon, R.A.** (2009). Transcriptome analysis of *Arabidopsis* wild-type and *gl3-sst sim* trichomes identifies four additional genes required for trichome development. Mol. Plant **2:** 803–822.

**Mathur, J.** (2005). The ARP2/3 complex: Giving plant cells a leading edge. Bioessays **27:** 377–387.

**Mathur, J., and Chua, N.H.** (2000). Microtubule stabilization leads to growth reorientation in *Arabidopsis* trichomes. Plant Cell **12:** 465–477.

**Mathur, J., Spielhofer, P., Kost, B., and Chua, N.** (1999). The actin cytoskeleton is required to elaborate and maintain spatial patterning during trichome cell morphogenesis in *Arabidopsis thaliana*. Development **126:** 5559–5568.

**Oppenheimer, D.G., Pollock, M.A., Vacik, J., Szymanski, D.B., Ericson, B., Feldmann, K., and Marks, M.D.** (1997). Essential role of a kinesin-like protein in *Arabidopsis* trichome morphogenesis. Proc. Natl. Acad. Sci. USA **94:** 6261–6266.

**Paredez, A.R., Somerville, C.R., and Ehrhardt, D.W.** (2006). Visualization of cellulose synthase demonstrates functional association with microtubules. Science **312:** 1491–1495.

**Petrásek, J., and Schwarzerová, K.** (2009). Actin and microtubule cytoskeleton interactions. Curr. Opin. Plant Biol. **12:** 728–734.

**Preston, R.D.** (1974). The Physical Biology of Plant Cell Walls. (London: Chapman & Hall).

**Saedler, R., Mathur, N., Srinivas, B.P., Kernebeck, B., Hülskamp, M., and Mathur, J.** (2004). Actin control over microtubules suggested by DISTORTED2 encoding the Arabidopsis ARPC2 subunit homolog. Plant Cell Physiol. **45:** 813–822.

**Samaj, J., Müller, J., Beck, M., Böhm, N., and Menzel, D.** (2006). Vesicular trafficking, cytoskeleton and signalling in root hairs and pollen tubes. Trends Plant Sci. **11:** 594–600.

**Sampathkumar, A., Lindeboom, J.J., Debolt, S., Gutierrez, R., Ehrhardt, D.W., Ketelaar, T., and Persson, S.** (2011). Live cell imaging reveals structural associations between the actin and microtubule cytoskeleton in *Arabidopsis*. Plant Cell **23:** 2302–2313.

**Schnittger, A., and Hülskamp, M.** (2002). Trichome morphogenesis: A cell-cycle perspective. Philos. Trans. R. Soc. Lond. B Biol. Sci. **357:** 823–826.

**Schulgasser, K., and Witztum, A.** (2004). The hierarchy of chirality. J. Theor. Biol. **230:** 281–288.

**Schwab, B., Mathur, J., Saedler, R., Schwarz, H., Frey, B., Scheidegger, C., and Hülskamp, M.** (2003). Regulation of cell expansion by the DISTORTED genes in *Arabidopsis thaliana*: Actin controls the spatial organization of microtubules. Mol. Genet. Genomics **269:** 350–360.

**Sheahan, M.B., Staiger, C.J., Rose, R.J., and McCurdy, D.W.** (2004). A green fluorescent protein fusion to actin-binding domain 2 of Arabidopsis fimbrin highlights new features of a dynamic actin cytoskeleton in live plant cells. Plant Physiol. **136:** 3968–3978.

**Smith, L.G., and Oppenheimer, D.G.** (2005). Spatial control of cell expansion by the plant cytoskeleton. Annu. Rev. Cell Dev. Biol. **21:** 271–295.

**Staiger, C.J., Sheahan, M.B., Khurana, P., Wang, X., McCurdy, D.W., and Blanchoin, L.** (2009). Actin filament dynamics are dominated by rapid growth and severing activity in the *Arabidopsis* cortical array. J. Cell Biol. **184:** 269–280.

**Stern, M.D., Aihara, H., Cho, K.H., Kim, G.T., Horiguchi, G., Roccaro, G. A., Guevara, E., Sun, H.H., Negeri, D., Tsukaya, H., and Nibu, Y.** (2007). Structurally related *Arabidopsis* ANGUSTIFOLIA is functionally distinct from the transcriptional corepressor CtBP. Dev. Genes Evol. **217:** 759–769.

**Stewart, J.M.** (1975). Fiber initiation on the cotton ovule (*Gossypium hirsutum*). Am. J. Bot. **62:** 723–730.

**Sugimoto, K., Williamson, R.E., and Wasteneys, G.O.** (2000). New techniques enable comparative analysis of microtubule orientation, wall texture, and growth rate in intact roots of *Arabidopsis*. Plant Physiol. **124:** 1493–1506.

**Szymanski, D.B.** (2005). Breaking the WAVE complex: The point of *Arabidopsis* trichomes. Curr. Opin. Plant Biol. **8:** 103–112.

**Szymanski, D.B.** (2009). Plant cells taking shape: New insights into cytoplasmic control. Curr. Opin. Plant Biol. **12:** 735–744.

**Szymanski, D.B., Marks, M.D., and Wick, S.M.** (1999). Organized F-actin is essential for normal trichome morphogenesis in *Arabidopsis*. Plant Cell **11:** 2331–2347.

**Takahashi, H., Hirota, K., Kawahara, A., Hayakawa, E., and Inoue, Y.** (2003). Randomization of cortical microtubules in root epidermal cells induces root hair initiation in lettuce (*Lactuca sativa* L.) seedlings. Plant Cell Physiol. **44:** 350–359.

**Tominaga-Wada, R., Ishida, T., and Wada, T.** (2011). New insights into the mechanism of development of Arabidopsis root hairs and trichomes. Int. Rev. Cell Mol. Biol. **286:** 67–106.

**Torres-Ruiz, R.A., and Jürgens, G.** (1994). Mutations in the *FASS* gene uncouple pattern formation and morphogenesis in *Arabidopsis* development. Development **120:** 2967–2978.

**Volkmann, N., Amann, K.J., Stoilova-McPhie, S., Egile, C., Winter, D.C., Hazelwood, L., Heuser, J.E., Li, R., Pollard, T.D., and Hanein, D.** (2001). Structure of Arp2/3 complex in its activated state and in actin filament branch junctions. Science **293:** 2456–2459.

**Wada, H.** (2012). Hierarchical helical order in the twisted growth of plant organs. Phys. Rev. Lett. **109:** 128104.

**Wightman, R., and Turner, S.R.** (2008). The roles of the cytoskeleton during cellulose deposition at the secondary cell wall. Plant J. **54:** 794–805.

**Xu, T., Qu, Z., Yang, X., Qin, X., Xiong, J., Wang, Y., Ren, D., and Liu, G.** (2009). A cotton kinesin GhKCH2 interacts with both microtubules and microfilaments. Biochem. J. **421:** 171–180.

**Zhang, C., Mallery, E.L., and Szymanski, D.B.** (2013). ARP2/3 localization in Arabidopsis leaf pavement cells: A diversity of intracellular pools and cytoskeletal interactions. Front. Plant Sci. **4:** 238.

**Zhang, X., Dyachok, J., Krishnakumar, S., Smith, L.G., and Oppenheimer, D.G.** (2005). IRREGULAR TRICHOME BRANCH1 in Arabidopsis encodes a plant homolog of the actin-related protein2/3 complex activator Scar/WAVE that regulates actin and microtubule organization. Plant Cell **17:** 2314–2326.